Engineering Analysis with Boundary Elements 35 (2011) 1237–1247

Contents lists available at ScienceDirect

Engineering Analysis with Boundary Elements

journal homepage: www.elsevier.com/locate/enganabound

Non-linear boundary element formulation applied to contact analysis using tangent operator

Edson Denner Leonel*, Wilson Sergio Venturini

University of São Paulo, School of Engineering of São Carlos, Department of Structural Engineering, Av. Trabalhador SãoCarlense, 400, 13.566–590 São Carlos-SP, Brazil

A R T I C L E I N F O

Article history:
Received 31 August 2010
Accepted 16 June 2011

Keywords:
Boundary element method
Contact problem
Non-linear formulation
Tangent operator

A B S T R A C T

This work presents a non-linear boundary element formulation applied to analysis of contact problems. The boundary element method (BEM) is known as a robust and accurate numerical technique to handle this type of problem, because the contact among the solids occurs along their boundaries. The proposed non-linear formulation is based on the use of singular or hyper-singular integral equations by BEM, for multi-region contact. When the contact occurs between crack surfaces, the formulation adopted is the dual version of BEM, in which singular and hyper-singular integral equations are defined along the opposite sides of the contact boundaries. The structural non-linear behaviour on the contact is considered using Coulomb's friction law. The non-linear formulation is based on the tangent operator in which one uses the derivate of the set of algebraic equations to construct the corrections for the non-linear process. This implicit formulation has shown accurate as the classical approach, however, it is faster to compute the solution. Examples of simple and multi-region contact problems are shown to illustrate the applicability of the proposed scheme.

1. Introduction

Contact mechanics is an important theme in the domain of solid mechanics. During the last few years, this theme has received an enormous attention from the scientific community due to its technological importance and complexity. The knowledge on the contact surface behaviour has great importance in mechanical, aeronautic and ship industry, where several forces are transferred among the solid parts using dents, connections and joints.

The boundary element method (BEM) is particularly suitable to handle this kind of analysis. As the discretization is required only along the boundary and contact surfaces, the number of degrees of freedom tends to be small in comparison with other numerical techniques as finite element method (FEM) and the extended finite element method (XFEM). However, this was not an impeditive to the development of some interesting formulations using these two last numerical methods. Friction and frictionless contact formulations for analysis of multi-bodies, crack surfaces and impact have been successfully developed using FEM [1–3] and XFEM [4,5].

To deal with complex contact problems, especially non-linear contact problems, BEM is recommended because this numerical method is capable to calculate accurately the values on body's boundary, where the contact occurs. In addition, the proposition of new BEM formulations for this problem is straightforward, because it gives explicit equations relating values prescribe and unknown on the boundary, including the surfaces in contact. Considering BEM to analyse contact problems appeared in the work due [6]. A contact BEM formulation based on the sub-region technique was proposed in [7] to analyse slope limit loads in geomechanic problems. They have developed and implemented a non-linear BEM formulation, using only singular integral equations, for which Mohr-Coulomb's criterion was assumed to define the collapse. The sub-region technique was also used by Man [8] and Aliabadi [9] for analysis of several types of contact problems, where linear and quadratic boundary elements were adopted. Coulomb's criterion was considered to model friction contact between cylindrical surfaces and crack lips by Gonzalez and Abascal [10] and Chen and Chen [11], respectively.

An automatic incremental technique was proposed by Huesmann and Kuhn [12], in which contact conditions change at only one node at the end of the increment, for two-dimensional elasto-plastic contact problems including friction. Their algorithm takes into account the elasto-plastic material behaviour over a fast iterative scheme. A BEM formulation applied to solve elastic frictional contact problems, using non-conforming discretization was presented in [13–15]. These formulations use singular and hyper-singular integral equations and the values on the contact surface are determined by enforcing tractions and displacements at every node of the contact zone with points on the opposite

* Corresponding author. Tel.: +55 163373 8211; fax: +55 163373 9482.
E-mail address: edleonel@sc.usp.br (E.D. Leonel).

0955-7997/$ - see front matter © 2011 Elsevier Ltd. All rights reserved.
doi:10.1016/j.enganabound.2011.06.005

surface. The frictional contact for 3-D problems was analysed in [16]. Their formulation was based on an incremental form considering constant triangular boundary elements. Some formulations for analysis of rolling contact were proposed by González and Abascal [17], Abascal and Rodríguez-Tembleque [18] and Rodríguez-Tembleque and Abascal [19]. These formulations were developed for analysis of 2D and 3D contact problems with BEM, allowing to consider real solid geometries and unstructured meshes. In addition, there is a normal and tangential cross-influence relation.

This paper proposes a non-linear BEM formulation using tangent operator to deal properly with contact problems. This implicit formulation is based on the use of only singular integral equations, only hyper-singular integral equations or singular plus hyper-singular integral equations, dual BEM [20], to model possible contacts that may appear among boundaries of different bodies and also between the crack surfaces introduced by crack propagation, as presented in [21,22]. In this last case, after the crack growth process, crack surfaces can close considering reversal loads and the new geometric structural configuration. The non-linear process is solved using a tangent operator, which is derived to assure better convergence and accuracy. This operator uses the derivate of the set of algebraic equations to construct the corrections on the non-linear process. This kind of operator has already been successfully used in the literature for dealing with many different engineering problems. For instance, [23,24] where localisation phenomenon and cohesive crack growth, respectively, were analysed. The derivation of this operator for contact problems using BEM is the main contribution of this paper. The tangent operator is derived considering Coulomb's friction criterion, which is adopted to govern the traction behaviour on the contact surfaces.

Examples of simple and multi-region contact problems are presented to illustrate the applicability and robustness of the proposed scheme. When possible, the results of the proposed BEM model are compared with FEM solution, based on ANSYS models. This formulation has shown accurate as the classical approach, however it is faster in terms of computational work.

2. Contact problem

In many types of structures, the applied external loads are transferred among the structural elements by the contact that occurs among them. Thus, the mechanical efficiency of the system depends on the nature of the interaction between the contact surfaces. Although this mechanical problem be very important for the industry, and many developments have already been made, many researches search for new models and improvements to simulate this problem. In practice, the knowledge on the contact problem can be improved using experience and observation. As the direct observation is often impossible, because the areas of interest are hidden under the contact surfaces, the mechanical behaviour has to be averaged along the contact surfaces. The parameters of interest to be measured in laboratory are the ultimate cohesive stresses and the friction angle, when Coulomb's friction law is assumed. These parameters can be used to evaluate the actual condition along the contact: stick (perfect coupling), slip or total separation.

Another important difficulty regarding the contact problem is that its behaviour is always dependent upon the involved materials, the surface texture, the topology, loading rate, the amount of applied load, the load direction, boundary conditions, among others. The friction contribution is almost always taken into account to evaluate the safety of mechanical system. Although, many times the friction contribution is not critical, the absence of knowledge on this effect can lead to unsafe and inefficient design.

2.1. Remarks on the friction effects

The physical mechanism of the friction can be seen as the strength to sliding between two contact surfaces. The cohesion between the contact surfaces is strongly influenced by their roughness and also by the material microstructure. The friction has enormous effects on the normal and shear traction interaction during the contact between the surfaces. Thus, an accurate solution is only possible if the friction is taken into account. Coulomb's friction law is the more often model assumed to represent the contact between two surfaces in engineering problems. This friction law defines that the sliding between two surfaces in contact occurs only when the shear traction, in absolute value at any surface point, is larger than the initial cohesion value plus the product between normal traction by the friction angle tangent, which represents the roughness between the surfaces. Moreover, the shear traction in the contact surfaces is governed by the following expression:

$$|\tau| \leq c_s - \sigma_n \tan(\phi) \tag{1}$$

where ϕ is the friction angle, σ_n is the traction component perpendicular to the contact surface (negative if compressive traction), τ is the traction component parallel to the contact surface and c_s is the cohesion.

Regarding Eq. (1), the contact between surfaces, considering friction effect among them, originates a non-linear problem due the dependency of normal and shear tractions in the contact surfaces. To solve properly this non-linear problem the incremental procedure with tangent operator is described in Section 4, which take into account positive and negative values for shear tractions in the contact surfaces.

The formulation proposed in this paper is capable to simulate contact problems according to the following modes separation: slip and stick. For each of these modes, the conditions below are assumed:

$$\begin{array}{lll}
\text{Separation} & \text{Slip} & \text{Stick} \\
\tau^{\ell}+\tau^{r}=0 & \tau^{\ell}+\tau^{r}=0 & \tau^{\ell}+\tau^{r}=0 \\
\sigma_n^{\ell}+\sigma_n^{r}=0 & \sigma_n^{\ell}+\sigma_n^{r}=0 & \sigma_n^{\ell}+\sigma_n^{r}=0 \\
\tau^{\ell}=0 & |\tau^{r}|=|\tau^{\ell}|=c_s-\sigma_n^{\ell}\tan\phi & u_t^{\ell}-u_t^{r}=0 \\
\sigma_n^{\ell}=0 & u_n^{\ell}-u_n^{r}=gap_n^{\ell r} & u_n^{\ell}-u_n^{r}=gap_n^{\ell r}
\end{array} \tag{2}$$

where the superscripts ℓ and r represent the left and right contact surface sides, respectively, the subscripts n and t indicate the normal and parallel directions of the contact surface, respectively, u is the displacements on the contact surface and $gap_n^{\ell r}$ indicates an initial gap between the contact surfaces before the application of the loads.

According to the active contact mode, the variables to be calculated in the contact surface change. Consequently, the equations used to analyse the problem also change. Therefore, the conditions presented in Eq. (2) coupled with algebraic BEM equations are used to construct the tangent operator in order to solve the non-linear problem and predict the contact values.

3. Boundary integral equations

In two-dimensional elasticity, the boundary integral equations can be obtained considering a homogeneous domain, Ω, with a boundary, Γ. The equilibrium equation can be written in terms of displacements as

$$u_{i,jj} + \frac{1}{1-2\upsilon} u_{j,ji} + \frac{b_i}{\mu} = 0 \tag{3}$$

where μ represents the shear elastic modulus, u_i gives the displacement components, b_i is the body forces and υ is Poisson's ratio.

This equilibrium representation can be transformed to an integral representation by applying Betti's reciprocity theorem or using weighted residual method. Considering these approaches, the integral representation written in terms of displacements is obtained

$$c_{il}(f,c)u_l(f)+\fint_{\Gamma} P^*_{il}(f,c)u_l(c)d\Gamma=\int_\Gamma P_l(c)u^*_{il}(f,c)d\Gamma \tag{4}$$

where u^*_{ij} and p^*_{ij} are Kelvin's fundamental solutions for displacement and tractions, respectively, u_j and p_j are boundary displacements and tractions, respectively, and c_{il} the well known free term for elastic problems; c_{il} is equal to δ_{il} for internal points, zero for outside points and $\delta_{il}/2$ for smooth boundary nodes and $\fint$ means integral of Cauchy principal value.

Eq. (4) is named in this paper as singular integral equation because of the singularity level of its kernels. Other important integral equation used in the proposed non-linear formulation is the hyper-singular integral equation. This integral equation, written in terms of tractions, can be obtained from Eq. (4), which must be differentiated to obtain the integral representation in terms of strains. Then, Hooke's law is applied to obtain the integral representation in terms of stresses. Finally, multiplication by the director cosines of the normal to crack surfaces at the collocation point leads to the traction representation, as follows:

$$\frac{1}{2}P_j(f)+\eta_k \fint_{\Gamma} S_{kj}(f,c)u_k(c)d\Gamma=\eta_k \fint_{\Gamma} D_{kj}(f,c)P_k(c)d\Gamma \tag{5}$$

where $\fint$ indicates finite part of Hadamard integrals; the kernels S_{kj} and D_{kj} are obtained from the kernels P^*_{ij} e u^*_{ij} by applying the definition of tractions.

To deal with crack problems using BEM, one of the most popular techniques is the dual boundary element method (DBEM) [20,21,25]. For DBEM, Eqs. (4) and (5) are used to obtain the algebraic relations for nodes defined along the boundary and crack surfaces. Eq. (4) is chosen to obtain the algebraic relations at nodes defined along the external boundary and along one crack surface, while Eq. (5) is used to obtain the algebraic relations at the opposite nodes, along the other crack surface.

This scheme has been widely used for analysis of crack propagation [21,24,25], although in this paper the objective is to apply it for analysis of pure contact between crack lips. Especially, contact surfaces, which are resulted from crack propagation. Besides DBEM, three other schemes to select algebraic equations are considered in order to deal properly with contact problems using BEM. These schemes are used for analysis of multi-bodies contact. They are based on the sub-region technique, in which each solid lead to a block of algebraic equations and then they are joined together by imposing equilibrium and displacement compatibility conditions. For the first scheme, only algebraic relations coming from the singular integral equation, Eq. (4), are used. This scheme is named as Singular Sub-region Technique—SST. The second idealised scheme is defined using along the external boundary only algebraic equations coming from the singular integral equation, Eq. (4), while along the contact surfaces only algebraic equations coming from the hyper-singular integral equation, Eq. (5), are used. This scheme is named in this paper as Hyper Singular Sub-region Technique—HST. An alternative scheme was also tested in which all the algebraic relations along the contact surfaces and along the boundary are written from the hyper-singular integral equation, Eq. (5). This scheme is named as Total Hyper-singular Sub-region Technique—THST.

The last three schemes above mentioned are more convenient to be used in solving pure contact problems. When they are used to analyse a contact problem coming from crack growth, an inconvenient remeshing procedure has to be used leading to a non-efficient computational algorithm regarding the required computer time consumption. Then, for problems involving cracks, the DBEM formulation is recommended.

It is worth to emphasise that when algebraic relations are obtained from Eq. (5), discontinuous elements must to be used to approximate tractions and displacements. As the hyper-singular integral equation can only be approximated if the derivates of the displacements are continuous in the vicinity of the source point, the nodes are defined inside the elements. On the contrary, continuous elements can be used along the boundary and along the contact surfaces. Considering SST approach, for instance, continuous elements can be adopted for all boundaries.

For the four schemes of equation selection described above, the algebraic equations are obtained from Eqs. (4) and (5) after dividing the boundary and the contact surfaces into elements along which displacements and tractions are approximated. These algebraic representations written for a convenient number of collocation points along the boundary and along the contact surfaces are split into two blocks of algebraic equations: equations written for boundary source nodes, equation written for contact source nodes.

For a selected number of boundary nodes, a block of algebraic equations are obtained relating boundary and contact values, as follows:

$$H^b_bU_b+H^c_bU_c=G^b_bP_b+G^c_bP_c \tag{6}$$

where U_b and U_c are displacements at the boundary nodes (b) and at contact surface nodes (c), respectively; P_b gives the boundary tractions, while P_c represents the tractions acting along the contact surfaces; H^b_b, H^c_b, G^b_b and G^c_b are the corresponding matrices to take into account displacement and traction effects; the subscript b indicates that the collocation point is at the boundary and the superscripts specify the boundary (b) or contact surface (c) values. For three schemes discussed before (DBEM, SST and HST), Eq. (6) is obtained using only Eq. (4). Nevertheless, as already commented before, the block of Eq. (6) may also be obtained from Eq. (5), as made for THST.

For the contact surfaces we need to define two opposite collocation points, one for each contact surface, to obtain four algebraic independent relations, corresponding to four unknown contact surface values, two displacements and two tractions. For these collocation points, the following block of algebraic is obtained:

$$H^b_cU_b+H^c_cU_c=G^b_cP_b+G^c_cP_c \tag{7}$$

where the subscript c in the matrices H^x_c and G^x_c indicates equation written for collocation points along the contact surfaces.

If the schemes HST and THST are adopted, Eq. (7) is constructed using only Eq. (5). On the other hand, if SST is used, Eq. (7) is evaluated using only Eq. (4). Finally, if DBEM is adopted Eq. (7) is computed using Eq. (4), for one contact surface, and Eq. (5), for the opposite contact surface.

The non-singular element integrals coming from Eq. (4) are evaluated using a Gauss–Legendre numerical scheme accomplished with a sub-element technique, while the singular element integrals are analytically evaluated. The integrals appearing in the Eq. (5) are calculated using analytical expressions. Based on these procedures, Eqs. (6) and (7) are evaluated with very low integration errors.

4. Non-linear solution technique using tangent operator

In this section, the non-linear BEM formulation using tangent operator applied to analysis of contact problems will be discussed. Firstly, the formulation for contact between crack surfaces is introduced. Afterwards, the formulation is extended to consider the case of multi-bodies contact. The use of tangent operators has demonstrated to be an interesting strategy in solving many non-linear problems. Using tangent operator to solve the non-linear system of algebraic equations in the context of BEM has shown to be an accurate and stable procedure in which convergence is achieved faster [23,24,26].

4.1. Tangent operator for contact between crack surfaces

Bearing in mind that the displacements and tractions at nodes belonging to the two opposite contact surfaces are independent, the equilibrium Eqs. (6) and (7) can be modified as follows:

$$H_b^b U_b + H_b^r U_r + H_b^\ell U_\ell = G_b^b P_b + G_b^r P_r + G_b^\ell P_\ell \tag{8}$$

$$H_c^b U_b + H_c^r U_r + H_c^\ell U_\ell = G_c^b P_b + G_c^r P_c^r + G_c^\ell P_\ell \tag{9}$$

where the subscripts r and ℓ are related to collocation points located at the right and left contact surfaces, respectively.

To obtain the expression of the tangent operator, Eqs. (8) and (9) have to be modified. Firstly, by transforming the contact surface displacement and traction vectors to local coordinates (n, s), in which n and s are coordinate axes perpendicular and parallel to the contact surfaces, respectively. The local coordinate system considered is illustrated in Fig. 1.

After this modification, these equations can be further modified by introducing the gap openings in the directions parallel and perpendicular to the contact surfaces, u_s and u_n, respectively. Thus, the displacement components associated with the left contact surface is replaced by

$$U_{\ell s} = u_s - U_{rs} \tag{10}$$

$$U_{\ell n} = u_n - U_{rn} \tag{11}$$

It is worth to emphasise that the contact condition, stick or slip, is considered active when $U_{\ell n} + U_{rn} + gap_n^{\ell r}$ is lesser or equal to zero. In this case structural interpenetration is observed and it must to be taken into account by BEM equations. Otherwise, if the condition above is positive, separation of contact surface is considered and the contact values are those presented in Eq. (2). Therefore, initial gap is considered in the formulation by only to determine the contact condition.

The equilibrium conditions have also to be applied in both, the tangential and normal directions, (Fig. 1), as follows:

$$-P_{\ell s} + P_{rs} = 0 \tag{12}$$

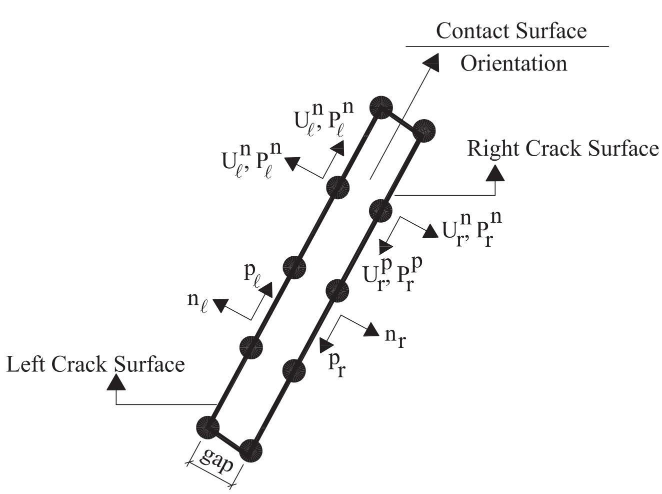

Fig. 1. Local coordinate system adopted for crack contact surfaces.

$$-P_{\ell n} + P_{rn} = 0 \tag{13}$$

Thus, after introducing the relations (10) to (13) into the blocks of algebraic Eqs. (8) and (9) one obtains

$$\begin{aligned} Y_b = {} & H_b^b U_b + [H_b^{rs} - H_b^{\ell s}] U_{rs} + [H_b^{rn} - H_b^{\ell n}] U_{rn} + H_b^{\ell s} u_s + H_b^{\ell n} u_n \\ & - G_b^b P_b - [G_b^{rs} + G_b^{\ell s}] P_{rs} - [G_b^{rn} + G_b^{\ell n}] P_{rn} \end{aligned} \tag{14}$$

$$\begin{aligned} Y_c = {} & H_c^b U_b + [H_c^{rs} - H_c^{\ell s}] U_{rs} + [H_c^{rn} - H_c^{\ell n}] U_{rn} + H_c^{\ell s} u_s + H_c^{\ell n} u_n \\ & - G_c^b P_b - [G_c^{rs} + G_c^{\ell s}] P_{rs} - [G_c^{rn} + G_c^{\ell n}] P_{rn} \end{aligned} \tag{15}$$

where the matrices H_x^{rs} and H_x^{rn} are obtained from H_x^r by computing the contribution due to the components U_{rs} and U_{rn}, respectively. Similarly, $H_x^{\ell s}$ and $H_x^{\ell n}$ are obtained from H_x^ℓ taking into account the contribution due to $U_{\ell s}$ and $U_{\ell n}$; G_x^{rs} and G_x^{rn} came from G_x^r, while $G_x^{\ell s}$ and $G_c^{\ell n}$ came from G_x^ℓ; the subscript x means b for Eq. (14) and c for Eq. (15). Y_b and Y_c are residual term related to boundary and contact collocation point position, respectively. These variables must be lesser than a specified tolerance to achieve the convergence.

Eqs. (14) and (15) compose a non-linear system of equations, considering contact problems, that must be properly solved. These equations are applied to any contact problem and depend only on the adopted non-linear contact criterion. To solve the equations above, the Newton–Raphson scheme was used with prevision and correction phases inside each load increment. Therefore, within a load step $\Delta t_n = t_{n+1} - t_n$ an iterative process is required to achieve the equilibrium. For any load step, Eqs. (14) and (15) have to be rewritten in terms of increments, i.e., the rate vector values have to be replaced by their increments: Δu_s, Δu_n, ΔU_{rs}, ΔU_{rn}, ΔP_{rs}, ΔP_{rn} and the unknowns values at the boundary, ΔX.

In this paper, the equilibrium configuration in each load step is achieved using a tangent operator. To obtain the terms of this operator, the Eqs. (14) and (15) must be expanded using Taylor's expansion. Taking into account only the first term of Taylor's expansion, these equations can be obtained as follows:

$$\begin{aligned} & Y(\Delta X^i, \Delta U_{rn}^i, \Delta U_{rs}^i, \Delta u_s^i, \Delta u_n^i, \Delta P_{rs}^i, \Delta P_{rn}^i) + \frac{\partial Y(\Delta X^i, \ldots)}{\partial \Delta X^i} \delta \Delta X^i \\ & + \frac{\partial Y(\ldots, \Delta u_s^i, \ldots)}{\partial \Delta u_s^i} \delta \Delta u_s^i + \frac{\partial Y(\ldots, \Delta u_n^i, \ldots)}{\partial \Delta u_n^i} \delta \Delta u_n^i + \frac{\partial Y(\ldots, \Delta U_{rs}^i, \ldots)}{\partial \Delta U_{rs}^i} \delta \Delta U_{rs}^i \\ & + \frac{\partial Y(\ldots, \Delta U_{rn}^i, \ldots)}{\partial \Delta U_{rn}^i} \delta \Delta U_{rn}^i + \frac{\partial Y(\ldots, \Delta P_{rs}^i, \ldots)}{\partial \Delta P_{rs}^i} \delta \Delta P_{rs}^i + \frac{\partial Y(\ldots, \Delta P_{rn}^i)}{\partial \Delta P_{rn}^i} \delta \Delta P_{rn}^i = 0 \end{aligned} \tag{16}$$

The terms multiplying the increments compose the tangent operator. Therefore, for the first try of the first load increment, stick contact mode is assumed. As a result, Δu_s and Δu_n are zero and consequently the system of algebraic equations is solved in terms of ΔP_{rs} and ΔP_{rn}. For this condition the structure is solved considering the follow system of equations:

$$\begin{Bmatrix} \Delta X \\ \Delta U_{rs} \\ \Delta U_{rn} \\ \Delta P_{rs} \\ \Delta P_{rn} \end{Bmatrix} = \begin{bmatrix} A \\ [H^{rs} - H^{\ell s}] \\ [H^{rn} - H^{\ell n}] \\ -[G^{rs} + G^{\ell s}] \\ -[G^{rn} + G^{\ell n}] \end{bmatrix}^{-1} \{\Delta F\} \tag{17}$$

The terms A and ΔF are obtained by applying the boundary conditions on the system of equations. All boundary equations associated with unknown variables were moved to A matrix. The vector ΔF is obtained by multiplying the boundary equations associated with known variables by the values prescribed on the boundary.

For the following iteration (k), the system of equations is solved using the Eqs. (14) and (15). However, the unknown variables depend on the contact conditions (contact mode) determined (active) at the end of the previous iteration ($k-1$). If stick mode is observed at the end of the previous iteration, $U_{\ell n}+U_{rn}+gap_n^{\ell r}=0$ and $|P_{rs}|<c_s-P_{rn}\tan(\phi)$, no sliding appears and the variables increments are evaluated considering the Eq. (17). In this case, the problem remains linear. As a result of evaluating Eq. (17), the tractions and displacements values at right contact surface and the unknown variables at the external boundary are obtained.

The sliding condition is observed when $U_{\ell n}+U_{rn}+gap_n^{\ell r}=0$ and Coulomb's friction law is not satisfied. In this case, the structural non-linear behaviour is introduced in the problem by the non-linearity traction behaviour on the contact surfaces. When sliding condition occurs, Eq. (17) has to be rewritten to take into account new unknown variables. Considering Coulomb's friction law to govern the tractions values on the contact surfaces, the dependence between the tractions on tangent and normal directions to contact surfaces is included in the analysis. For this situation, the non-linear problem is solved using the tangent operator. Including Coulomb's law in Eqs. (14) and (15), the problem is solved by

$$\begin{Bmatrix} \Delta X \\ \Delta U_{rs} \\ \Delta U_{rn} \\ \Delta u_s \\ \Delta P_{rn} \end{Bmatrix} = \begin{bmatrix} A \\ [H^{rs}-H^{\ell s}] \\ [H^{rn}-H^{\ell n}] \\ H^{\ell s} \\ -[G^{rn}+G^{\ell n}]-[G^{rs}+G^{\ell s}](\partial P_s/\partial P_n) \end{bmatrix}^{-1} \{\Delta\hat{F}\} \tag{18}$$

where $\Delta\hat{F}$represents the vector with non-equilibrated forces, $(\partial P_s/\partial P_n)$ means the variation of tangential tractions on normal tractions at the contact surfaces. This term is obtained using Coulomb's friction law expression. Considering this law, this term becomes v $(\partial P_s/\partial P_n)=\tan(\phi)$. The matrix multiplying vector $\Delta\hat{F}$ is known as tangent operator, because it takes into account the variation of the non-linear contact law in the system of equations.

When the non-linear Coulomb's criterion is triggered, the tangent operator is constant. Therefore, it requires only one iteration to reach the equilibrium configuration at each load step. Of course, this is the situation where no change occurs in the contact conditions (modes) from one iteration to the next. If the contact mode changes at any collocation point, from one iteration to the next, the tangent operator, Eq. (18) has to be modified and complementary iterations are needed.

Thus, for contact problems where the surfaces in contact are easily identified, this formulation can be successfully applied. Special interest is addressed to contact between crack lips and also among soil and rock layers.

4.2. Tangent operator for multi-bodies contact

In this sub-section, the tangent operator formulation is extended to multi-bodies contact problems. Therefore, this formulation is applied to analysis of contact among interfaces of different materials that compose a structural system. To develop this formulation, the sub-region technique was adopted. Therefore, the displacement and traction compatibility along the contact surfaces are enforced for stick contact mode. Otherwise, in slip mode, the parallel components of displacements are leaving to slide on each other.

The contact condition is achieved when structural interpenetration is observed, i.e, when adding the normal displacements on each contact surface and the initial gap be lesser than or equal to zero. Otherwise, when structural interpenetration is not observed, separation model is considered. In this case, the nodes defined along the contact surfaces are treated independently, therefore with unknown displacements and prescribed traction when pressure is applied inside the gap opening.

Considering the different schemes of integral equations choice (SST, HST and THST), the BEM algebraic equations are calculated taking into account the sub-region technique as follows:

$$\sum_{i=1}^{Nd} H^{ii}U^i = \sum_{i=1}^{Nd} G^{ii}P^i \tag{19}$$

where Nd is the number of sub-domains in the analysis. Eq. (19) can be rewritten considering the collocation point localisation. These points are separated in collocation points belonging to external boundary and to contact boundary

$$\sum_{i=1}^{Ndn} H^iU^i + \sum_{j=1}^{Ndc} H^jU^j = \sum_{i=1}^{Ndn} G^iP^i + \sum_{j=1}^{Ndc} G^jP^j \tag{20}$$

where Ndn means the number of collocation points on the external boundaries and Ndc the number of collocation points on the contact boundaries.

We can further modify Eq. (20) by splitting the values on the contact boundaries. These values are described in terms of a local coordinates n and s normal and parallel directions to the contact surfaces, respectively, as illustrated in Fig. 1. After this modification, the values on the contact boundaries are described considering the right, r, and left, ℓ, position on the contact surface:

$$\begin{aligned}\sum_{i=1}^{Ndn} H^iU^i + \sum_{k=1}^{Nic}\left(\sum_{j=1}^{Ndc^k} H^j_{rs}U^j_{rs} + \sum_{j=1}^{Ndc^k} H^j_{rn}U^j_{rn} + \sum_{j=1}^{Ndc^k} H^j_{\ell s}U^j_{\ell s} + \sum_{j=1}^{Ndc^k} H^j_{\ell n}U^j_{\ell n}\right)_k \\ = \sum_{i=1}^{Ndn} G^iP^i + \sum_{k=1}^{Nic}\left(\sum_{j=1}^{Ndc^k} G^j_{rs}P^j_{rs} + \sum_{j=1}^{Ndc^k} G^j_{rn}P^j_{rn} + \sum_{j=1}^{Ndc^k} G^j_{\ell s}P^j_{\ell s} + \sum_{j=1}^{Ndc^k} G^j_{\ell n}P^j_{\ell n}\right)_k\end{aligned} \tag{21}$$

where Nic is the number of interface or contact surfaces.

Eq. (21) can be modified considering the values prescribed and unknowns on the external boundaries. Coupling the knows and unknowns values one has:

$$\begin{aligned}Y(U,P,X,F) = \sum_{i=1}^{Ndn} A^iX^i + \sum_{k=1}^{Nic}\left(\sum_{j=1}^{Ndc^k} H^j_{rs}U^j_{rs} + \sum_{j=1}^{Ndc^k} H^j_{rn}U^j_{rn} + \sum_{j=1}^{Ndc^k} H^j_{\ell s}U^j_{\ell s}\right. \\ \left. + \sum_{j=1}^{Ndc^k} H^j_{\ell n}U^j_{\ell n}\right)_k - F - \sum_{k=1}^{Nic}\left(\sum_{j=1}^{Ndc^k} G^j_{rs}P^j_{rs} + \sum_{j=1}^{Ndc^k} G^j_{rn}P^j_{rn}\right. \\ \left. + \sum_{j=1}^{Ndc^k} G^j_{\ell s}P^j_{\ell s} + \sum_{j=1}^{Ndc^k} G^j_{\ell n}P^j_{\ell n}\right)_k\end{aligned} \tag{22}$$

The A^i matrices are composed by all boundary algebraic equations of unknown variables. The vector F is obtained by multiplying the boundary algebraic equations of the known variables by the values applied at the boundary.

Considering this formulation for contact among multi-bodies, three possible contact modes may appear: stick, slip (sliding contact) and separation (no contact), Eq. (2). Regarding the first contact mode, the compatibility and equilibrium conditions have to be imposed on the values on contact boundaries, which are expressed as

$$U_\ell + U_r = 0 \quad \text{and} \quad -P_\ell + P_r = 0 \tag{23}$$

Thus, introducing Eq. (23) in Eq. (22), all values of displacements and tractions for the left contact surface side can be replaced

$$Y(U,P,X,F)=\sum_{i=1}^{Ndn}A^iX^i+\sum_{k=1}^{Nic}\left[\sum_{j=1}^{Ndc^k}(H_{rs}^j-H_{\ell s}^j)U_{rs}^j+\sum_{j=1}^{Ndc^k}(H_{rn}^j-H_{\ell n}^j)U_{rn}^j\right]_k$$
$$-F-\sum_{k=1}^{Nic}\left[\sum_{j=1}^{Ndc^k}(G_{rs}^j+G_{\ell s}^j)P_{rs}^j+\sum_{j=1}^{Ndc^k}(G_{rn}^j+G_{\ell n}^j)P_{rn}^j\right]_k \quad (24)$$

To solve properly the contact problem, the Newton–Raphson scheme was used considering prevision and correction phases inside each load increment. Consequently, Eq. (24) has to be solved by increments. For stick contact mode the increments on boundary values is evaluated using the equation

$$\begin{Bmatrix}\Delta X\\ \Delta U_{rs}\\ \Delta U_{rn}\\ \Delta P_{rs}\\ \Delta P_{rn}\end{Bmatrix}=\begin{bmatrix}\sum_{i=1}^{Ndn}A^i\\ \sum_{k=1}^{Nic}\left[\sum_{j=1}^{Ndc^k}(H_{rs}^j-H_{\ell s}^j)\right]_k\\ \sum_{k=1}^{Nic}\left[\sum_{j=1}^{Ndc^k}(H_{rn}^j-H_{\ell n}^j)\right]_k\\ -\sum_{k=1}^{Nic}\left[\sum_{j=1}^{Ndc^k}(G_{rs}^j+G_{\ell s}^j)\right]_k\\ -\sum_{k=1}^{Nic}\left[\sum_{j=1}^{Ndc^k}(G_{rn}^j+G_{\ell n}^j)\right]_k\end{bmatrix}^{-1}\{\Delta F\} \quad (25)$$

Eq. (25) represents a linear system of equations where tractions and displacements increments on the boundaries are calculated. As discussed at the beginning of this section, the stick contact mode is active when the sum among the normal displacements on each contact surface and the initial gap be lesser than or equal to zero. This condition depends on the equilibrium configuration determined in the previous step.

The second contact mode is addressed to modelling the sliding between the contact surfaces and slip mode. In this case, the tractions along the contact surfaces are evaluated considering Coulomb's friction law. Consequently, introducing this criterion into the formulation, the structural non-linear behaviour is included in the analysis.

To model the non-linear behaviour due the contact, the tangent operator was adopted to solve the non-linear equations. To derivate its terms, new unknown variables have to be considered in order to take into account sliding mode. Introducing compatibility and equilibrium conditions one has

$$U_{\ell n}+U_{rn}=0 \quad \text{and} \; -P_\ell+P_r=0 \quad (26)$$

Considering the conditions expressed by Eq. (26) and introducing Coulomb's law, Eq. (22) can be rewritten as

$$Y(U,P,X,F)=\sum_{i=1}^{Ndn}A^iX^i+\sum_{k=1}^{Nic}\left[\sum_{j=1}^{Ndc^k}H_{rs}^jU_{rs}^j+\sum_{j=1}^{Ndc^k}H_{\ell s}^jU_{\ell s}^j\right.$$
$$\left.+\sum_{j=1}^{Ndc^k}(H_{rn}^j-H_{\ell n}^j)U_{rn}^j\right]_k-F-\sum_{k=1}^{Nic}\left\{\sum_{j=1}^{Ndc^k}[(G_{rs}^j+G_{\ell s}^j)]P_{rs(P_{rn}^j)}^j\right.$$
$$\left.+\sum_{j=1}^{Ndc^k}[(G_{rn}^j+G_{\ell n}^j)]P_{rn}^j\right\}_k \quad (27)$$

The terms of the tangent operator are obtained using Taylor's expansion, as presented in Eq. (16). Expanding the terms of Eq. (27) and using Eq. (16) with only the first term of Taylor's expansion, the non-linear system is solved according the equation

$$\begin{Bmatrix}\Delta X\\ \Delta U_{rs}\\ \Delta U_{\ell s}\\ \Delta U_{rn}\\ \Delta P_{rn}\end{Bmatrix}=\begin{bmatrix}\sum_{i=1}^{Ndn}A^i\\ \sum_{k=1}^{Nic}\left[\sum_{j=1}^{Ndc^k}H_{rs}^j\right]_k\\ \sum_{k=1}^{Nic}\left[\sum_{j=1}^{Ndc^k}H_{\ell s}^j\right]_k\\ \sum_{k=1}^{Nic}\left[\sum_{j=1}^{Ndc^k}(H_{rn}^j-H_{\ell n}^j)\right]_k\\ -\sum_{k=1}^{Nic}\left[\sum_{j=1}^{Ndc^k}(G_{rn}^j+G_{\ell n}^j)-(G_{rs}^j+G_{\ell s}^j)(\partial P_s/\partial P_n)\right]_k\end{bmatrix}^{-1}\{\Delta\hat{F}\} \quad (28)$$

where $\Delta\hat{F}$ represents the vector with non-equilibrated forces, $(\partial P_s/\partial P_n)=\tan(\phi)$ indicates the variation of tractions according the tangential and normal directions to the contact surfaces. The matrix multiplying the vector $\Delta\hat{F}$ is known as tangent operator, because it takes into account the variation of the non-linear contact law into the system of equations.

The third contact mode, separation, is straightforward considered with this formulation. When this contact mode is observed, it means that the tractions and displacements on the contact surface are independent. Consequently, the collocation points on the contact boundary can be considered as external boundary and its algebraic equations are included in matrix A.

It is worth mentioning that using the non-linear Coulomb's friction law, the tangent operator is constant. Then, the non-linear process may achieve the convergence using only one iteration. This situation is observed when no change occurs in the contact conditions from one iteration to the next.

5. Applications

In this section, the proposed BEM contact formulation is used for the analysis of four examples. The first example addresses to analysis of a panel with a side crack in frictionless contact. The same structure is also analysed in the second application, where a friction contact is considered. In this last analysis, the load conditions and the contact parameters were changed. The third application presents a problem of two bodies contact. Finally, the last application deals with an analysis of a multi-body contact. In these applications, the results of the proposed formulations were compared with the responses of equivalent models constructed using ANSYS.

5.1. Panel with side crack. frictionless case

A square domain with side lengths of 2.0 m, presented in Fig. 2 is analysed. A crack of 1.0 m length starts at a middle point along the left vertical side. The displacement components are assumed zero along the lower side, while along the upper side, the displacements components prescribed are: u_x= 0.001 m and u_y= 0.001 m. Young's modulus E=1.000 kN/m^2 and Poison's ratio ν=0.2 were assumed, while the friction angle and the cohesion ultimate strength are zero.

The DBEM formulation was adopted for this analysis. The other alternatives discussed in the paper are not suitable to solve this problem. The results obtained with the proposed BEM formulation are compared with the solution given by the finite element code ANSYS. For the BEM analysis, 32 linear boundary elements were used while in ANSYS analysis the solid was discretized by 1600^2 and uniform finite elements. The displacements and tractions along the contact were compared using BEM and FEM

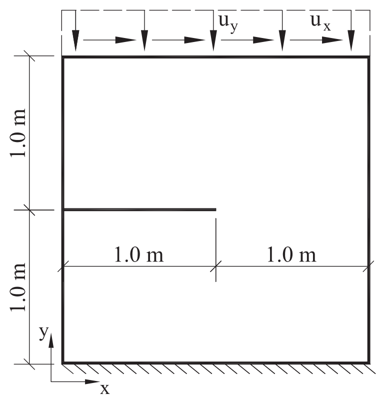

Fig. 2. Square domain with a side crack.

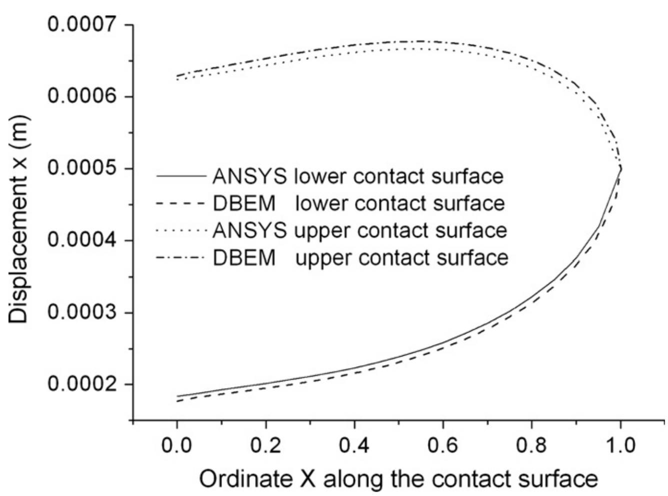

Fig. 3. Displacements in the direction *X*.

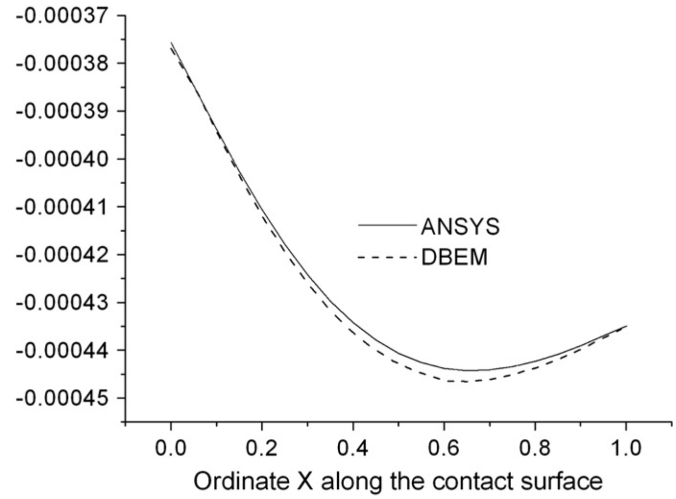

Fig. 4. Displacements in the direction *Y*.

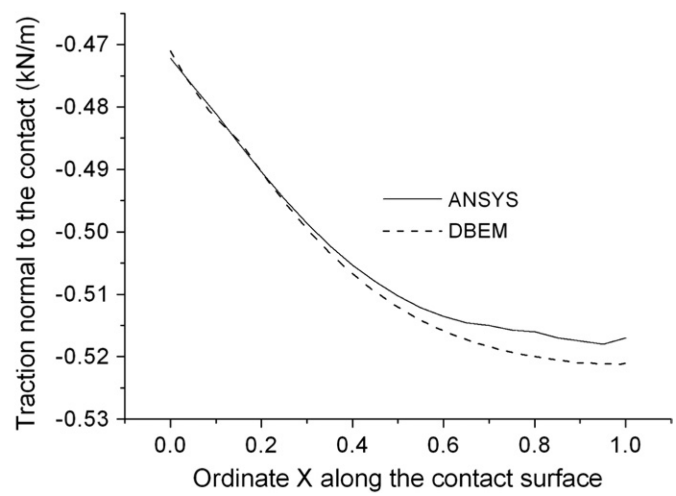

Fig. 5. Tractions along the contact surface in the direction *Y*.

approaches. The displacement results are presented in Figs. 3 and 4. Fig. 3 illustrates a good agreement between DBEM and ANSYS/FEM results for displacement components in the direction *X*. In the same way, the agreement between DBEM and ANSYS/FEM results are also observed in the *Y*-direction displacement components, shown in (Fig. 4).

The normal traction values along the contact surface were also compared (Fig. 5). As obtained for the displacement results, good agreement was also observed between DBEM and ANSYS/FEM results for the contact values. Thus, this example confirms the accuracy of the developed formulation.

5.2. *Panel with side crack. friction case*

The same domain analysed in the previous example was again studied, but now assuming a contact with friction. The boundary conditions presented in Fig. 2 were assumed with prescribed displacements along the upper side equal to $u_x = 0.05$ m and $u_y = 0.01$ m. The material parameters were also maintained: Young's modulus $E = 1.000$ kN/m^2 and Poison's ratio $\nu = 0.2$. The example is now analysed assuming a friction angle of $\varphi = 30^\circ$, along the crack surfaces, and a cohesive parameter of $c_s = 0$. Again, as the contact surface does not separate the body into two or more sub-regions, the DBEM was the only tested scheme.

The results for displacements and tractions along the contact surfaces were compared. Firstly, the results for the displacement component in the direction *X* was calculated using the proposed BEM formulation and the FEM model constructed in ANSYS are compared. Fig. 6 presents the curves obtained, in which a good agreement between the two numerical solutions can be observed. Fig. 7 confirms the agreement when displacement component in the direction *Y* is compared.

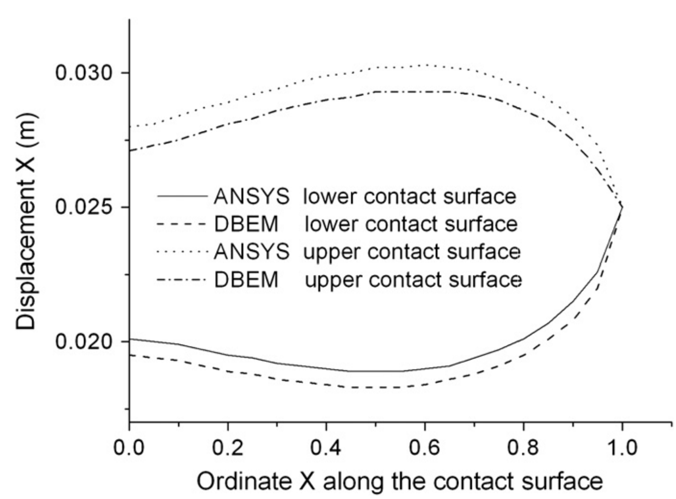

Fig. 6. Displacements in the direction *X*.

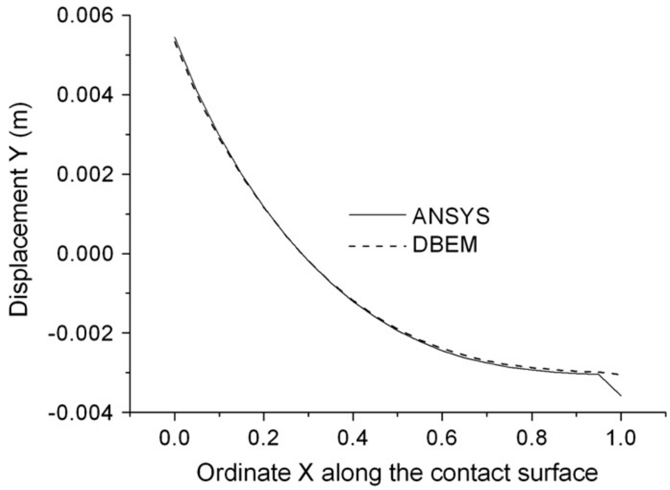

Fig. 7. Displacements in the direction *Y*.

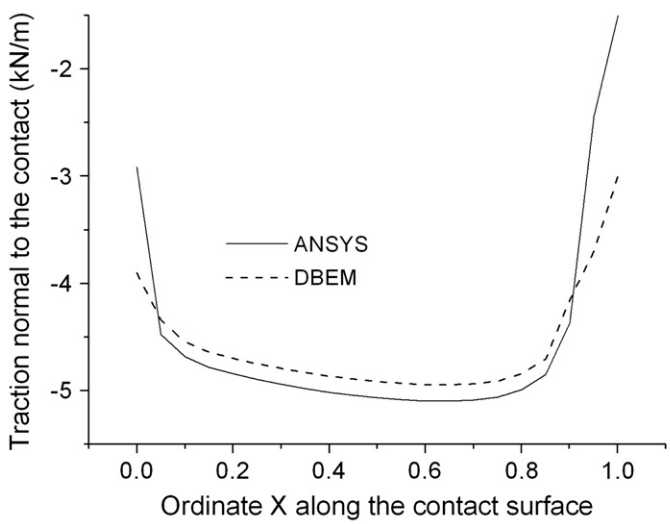

Fig. 8. Tractions along the contact surface in the direction *Y*.

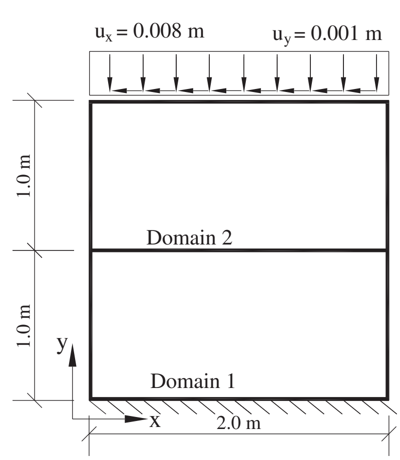

Fig. 9. Structure analysed: dimensions and boundary conditions.

The comparison between the traction results is given in Fig. 8. As expected, the results obtained using ANSYS/FEM and BEM compares well. Thus, this example, in which friction is taken into account, also demonstrated the accuracy of the proposed BEM formulation, with tangent operator, to model contact problems.

5.3. Contact between two blocks

The square structure formed by two blocks illustrated in Fig. 9 is analysed using the proposed BEM formulation. The four alternatives of choosing the algebraic equations were tested: (a) using

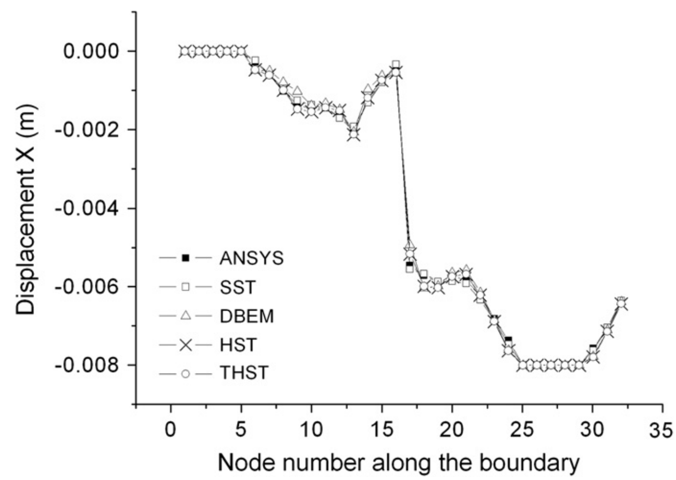

Fig. 10. Displacement in the direction *X* along all structural boundaries.

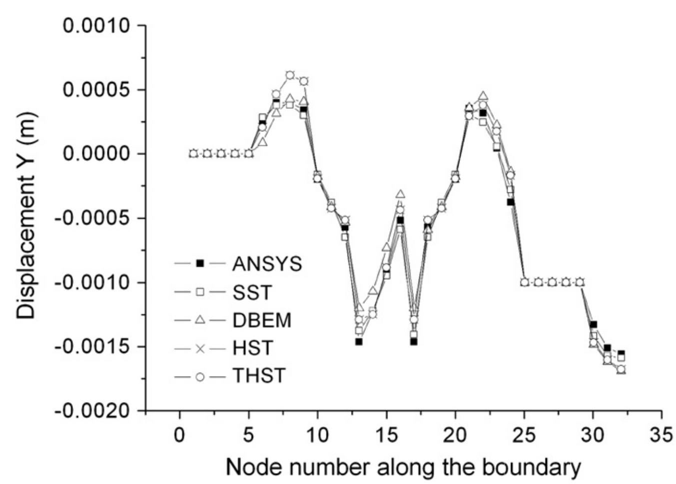

Fig. 11. Displacement in the direction *Y* along all structural boundaries.

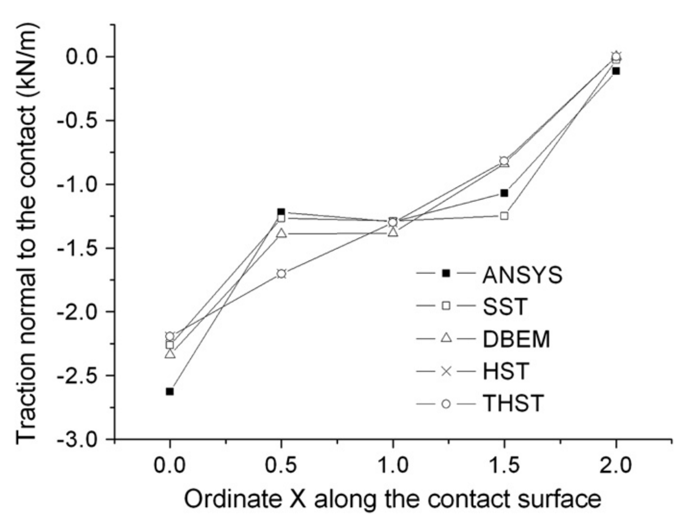

Fig. 12. Contact traction, along direction *Y*.

only singular equations (SST); (b) using singular equations along the boundary and singular plus hyper-singular equations along the contact (DBEM); and (c) using singular equations along the boundary and only hyper-singular equations along the contact (HST). The scheme which only hyper-singular equations are used, along the contact and along the boundary (THST), was also tested. These solutions were compared with the results obtained using ANSYS where an equivalent model was constructed using FEM.

The dimension adopted for the two blocks are given in Fig. 9 as well as the boundary conditions. Thus, the contact behaviour will be analysed when displacements are applied along the upper boundary. The properties for the two blocks are: block-1: Young's modulus equal to $E_1=3.0\times10^3$ kN/m^2 and Poisson's ratio $v_1=0.2$; block-2: Young's modulus equal to $E_2=2.0\times10^3$ kN/m^2 and Poisson's ratio $v_2=0.3$. Along the contact no cohesion is assumed, while the friction angle is 45°. Considering the BEM analysis, 32 linear boundary elements were used while in ANSYS analysis the structure was discretized by 1600^2 and uniform finite elements.

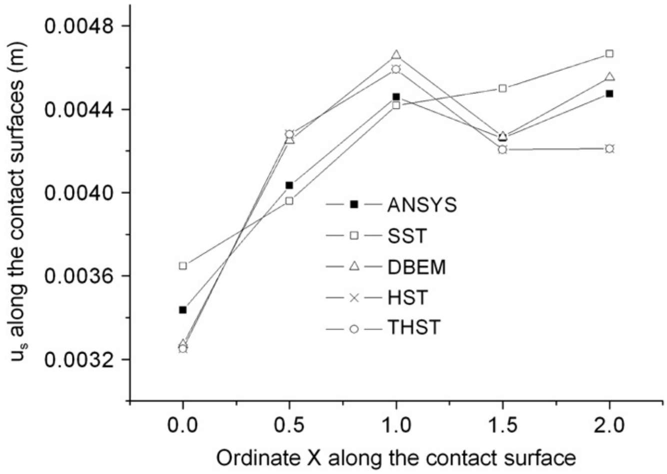

Fig. 13. u_s calculated between the contact surfaces.

The results in terms of displacement in the direction *X* is shown in Fig. 10, while Fig. 11 presents the displacement component in the direction *Y*. For these figures, the displacements are illustrated along all structural boundaries according the node numeration. The nodes are numbered in anticlockwise mode starting from the left lower corner, in which domain. The domain 1 is firstly numbered, nodes number 1–16, where nodes 9–13 belong to contact region. Then, the domain 2 is numbered, nodes number 17–32. The nodes 17–21 are positioned at the contact region. The results obtained using only singular equations (SST) are almost the same ones calculated by ANSYS/FEM approach. Considering this algebraic equations choice, the BEM model was capable to fit the FEM response for all boundaries. Using DBEM, i.e., using singular plus hyper-singular equations along the contact also presented excellent results. For this case, only small differences at few nodes were observed. Considering these two schemes for choosing the algebraic equations good agreement was observed with ANSYS/FEM. The results were not so accurate, when compared with ANSYS, SST and DBEM responses, for the case in which only hyper-singular equations are used along the contact surfaces and preserving singular equations for the boundary nodes (HST). Similar results were obtained when only hyper-singular equations are used along the boundary and contact surfaces (THST). For these two last schemes, the values at the contact region are correctly evaluated. However, for some nodes out of contact, small differences were observed.

The accuracy of the solution using the four selected schemes can also be verified by the traction profile, along the direction *Y*, presented in Fig. 12. As observed for the displacements behaviour analysis, the results obtained using only singular equations are accurate assuming ANSYS/FEM solution as reference. The DBEM gives still good results, but less accurate in comparison with SST scheme for some nodes. Using only hyper-singular equations along the contact surfaces (HST) and only hyper-singular equations along the contact surfaces and the boundary (THST) lead also to acceptable results in comparison with ANSYS/FEM. In spite of the accuracy observed, these two last approaches are lesser capable to fit the ANSYS/FEM results than SST and DBEM schemes.

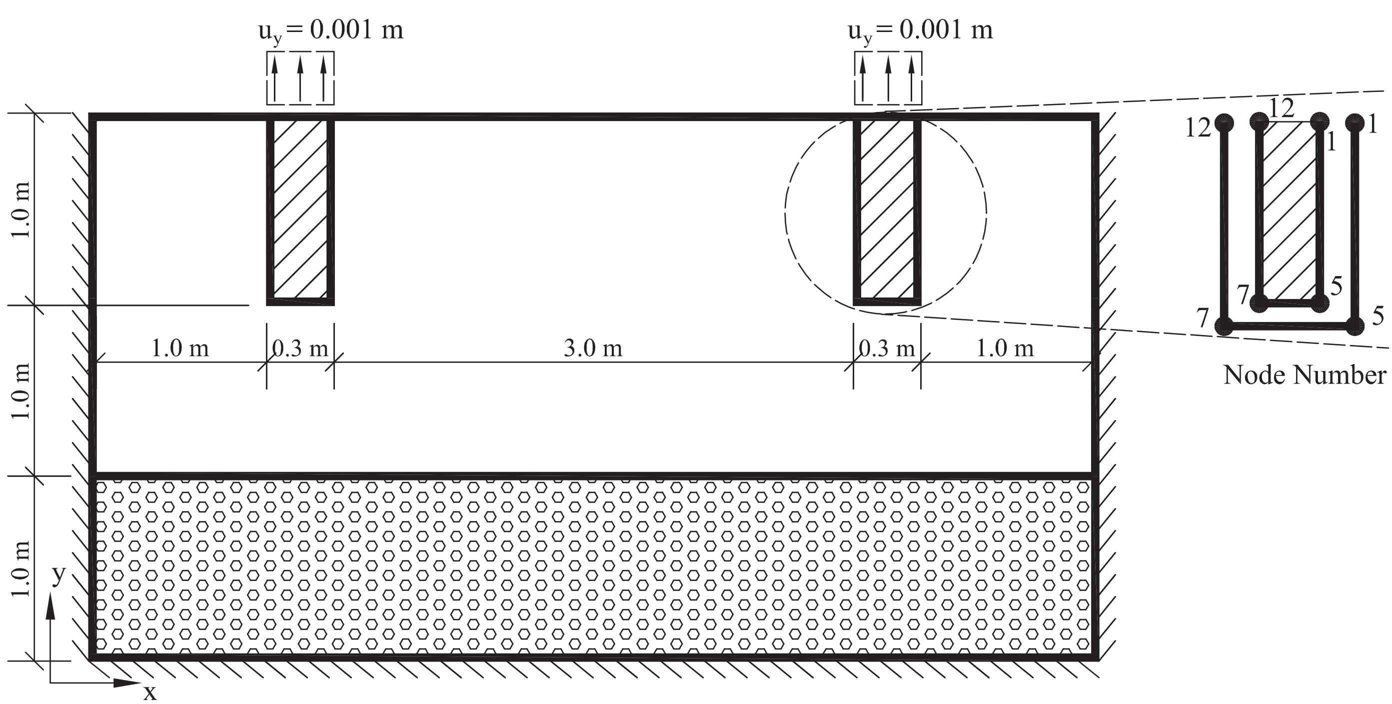

Fig. 14. Analysed domain: dimensions and boundary conditions.

The relative displacement u_s, parallel to the contact surface, is illustrated in Fig. 13. According this figure, the sliding between the surfaces in contact was observed (slip mode). This condition was achieved by all numerical approaches used in this analysis, along whole contact surfaces. The BEM schemes used were capable to fit, with considerable accuracy, the curve obtained by ANSYS/FEM, which was considered as reference. The results obtained in this example demonstrate that the proposed BEM formulation, with tangent operator, can be applied to model contact among bodies' boundaries. Especially, the models SST and DBEM, which have given accurate results for the values along the external boundary and contact surface.

5.4. Four sub-domain problem. multi-boundaries contact

In this example a more complex domain is analysed. The major structure is given by two layers. Two inclusions are embedded in the upper layer as presented in Fig. 14. The relevant dimensions together with the boundary conditions are given in the same figure. Displacements equal to zero are prescribed along the lower and vertical sides. The load is given by applying vertical displacements equal to 0.001 m along the top side of the two inclusions. The following material parameters have been adopted for the four sub-domains: domain 1, the lower rectangle, Young's modulus and Poisson's ratio are $E=2.5\times10^3$ kN/m^2 and $\nu=0.2$; domain 2, the upper rectangle, Young's modulus and Poisson's ratio $E=2.1\times10^3$ kN/m^2 and $\nu=0.3$; for the two inclusions Young's modulus and Poisson's ratio are $E=3.0\times10^3$ kN/m^2 and $\nu=0.15$, respectively. The cohesion between the two layers is $c_s=3.0\times10^5$ kN/m^2, while between the largest layer and the inclusions this value is equal to $c_s=1.0\times10^3$ kN/m^2. The friction angles are 45° and 30° for the contact between the two layers and between the upper layer and the inclusions, respectively. To discretise the whole body, 215 linear boundary and interface boundary elements were used.

This composed domain is analysed using three schemes for choosing algebraic equations discussed before: SST, DBEM and HST. Firstly, the displacements calculated along the contact surfaces between the upper rectangle and the inclusions are analysed. Fig. 15 presents the displacement results, in the direction Y, for the nodes belonging to the upper rectangle along the contact surface with the inclusion, while Fig. 16 shows the same results for the nodes belonging to the inclusion in the same contact interface. Only the results for the right inclusion were presented because symmetric behaviour was verified. The node

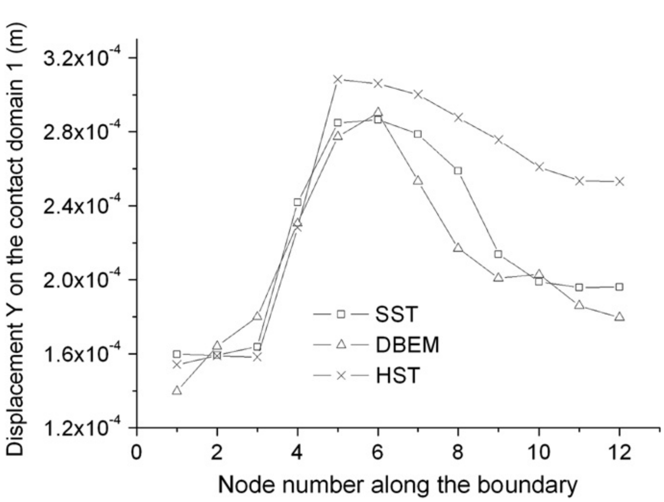

Fig. 15. Displacements in the direction Y calculated for the upper layer boundary.

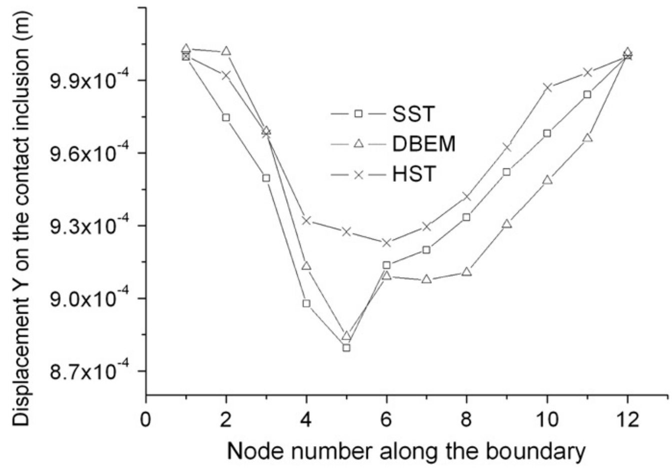

Fig. 16. Displacements in the direction Y calculated for the inclusion boundary.

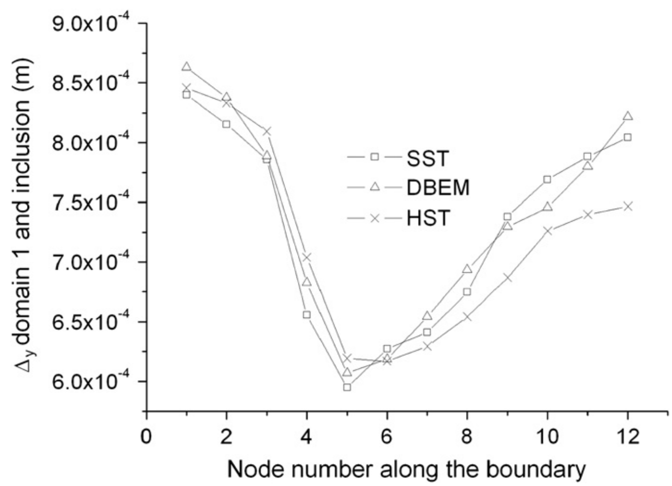

Fig. 17. Relative displacement among contact surfaces of domain 1 and inclusion.

numbering considered for the upper layer and the inclusion is presented in Fig. 14. The results obtained by the three equation selection schemes can be compared among them. According these two last figures, one can observe that similar results were achieved by SST and DBEM schemes, while HST scheme leads to small differences for some nodes, when compared with SST and DBEM. In spite of these small differences, a good agreement among the results was observed.

The results shown in these two last figures can be also used to analyse the sliding behaviour along the surfaces in contact. By subtracting the displacements illustrated in Fig. 16 from those presented in Fig. 15 is possible to determine the relative displacement in the direction Y, (Δ_y), among the surfaces in contact. This result is shown in Fig. 17, where one can observe that sliding (nodes 1–5 and 7–12) occurred, in the same way that debonding (nodes 5–7). This behaviour is also confirmed by the traction values, in parallel direction to the contact surfaces, among the upper layer and the right inclusion.

According the results presented in Figs. 17 and 18, no important differences were observed among the responses achieved by SST, DBEM and HST models. These models presented a good agreement among them for the values considered in this analysis. Then, it confirms that the tangent operator is an interesting alternative for dealing with non-linear problems.

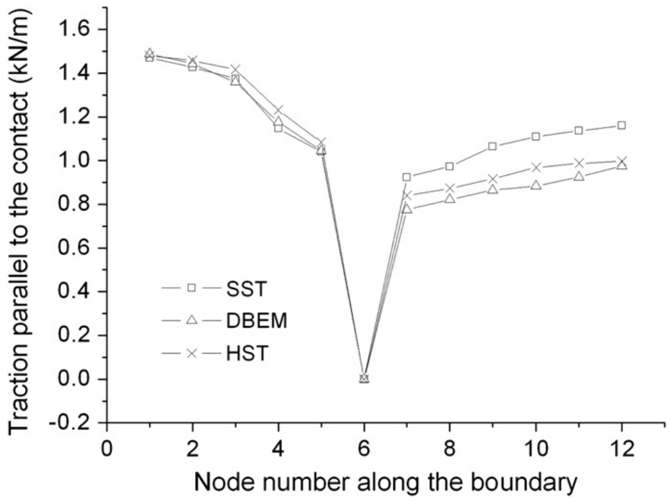

Fig. 18. Traction values in parallel direction to contact surfaces of domain 1 and inclusion.

6. Conclusions

The boundary element method has been applied to solve non-linear contact problems in this paper. A BEM formulation based on the use of a tangent operator was proposed to solve this complex engineering problem. Each term of the tangent operator, considering the contact between crack surfaces and among bodies' interfaces, was derived for the particular case of Coulomb's friction criterion. Four schemes to choice integral equations were used. According the results shown in this paper, especially those presented in item 5.3, the model that uses only algebraic equations coming from singular integral representation (SST) has demonstrated to be the more accurate when compared with a numerical reference. The dual boundary element method (DBEM) has also shown appropriate to deal with contact problems. Considering the case of contact between crack surfaces, this formulation has been capable to solve accurately the non-linear problem and to determine the boundary values.

The responses of the proposed formulation were compared with the results of equivalent models constructed using ANSYS (FEM). This comparative shows a good performance of the proposed BEM schemes, especially SST and DBEM. HST and THST schemes also led to acceptable results. However, for some nodes considered in the comparison, small differences were observed. It may occur due the singularity level present in the algebraic equations of these schemes, which is higher than the observed in SST and DBEM.

It is important to emphasise that using tangent operator requires a low number of iterations to achieve the convergence. Therefore, cumulating numerical errors due the iterations are avoided. As the tangent operator is constant, for the case of Coulomb's friction law, the correction step can be performed using only one iteration. Then, this formulation is efficient in terms of computational performance.

Although not shown in this paper, the formulation proposed is also efficient when dealing with problems containing several cracks already opened.

Acknowledgements

Sponsorship of this research project by the São Paulo State Foundation for Research – FAPESP – is greatly acknowledged.

References

[1] Lin T, Ou H, Runfang L. A finite element method for 3D static and dynamic contact/impact analysis of gear drives. Computer Methods in Applied Mechanics and Engineering 2007;196:1716–28.
[2] Tsai CT, Shankar M. Elasto-plastic finite element analysis of fretting stresses in pre-stressed strip in contact with cylindrical pad. Finite Elements in Analysis and Design 2000;36:171–87.
[3] Ko PL, Lyer SS, Vaughan H, Gadala M. Finite element modelling of crack growth and wear particle formation in sliding contact. Wear 2001;251: 1265–78.
[4] Khoei AR, Shamloo A, Azami AR. Extended finite element method in plasticity forming of powder compaction with contact friction. International Journal of Solids and Structures 2006;43:5421–48.
[5] Khoei AR, Nikbakht M. An enriched finite element algorithm for numerical computation of contact friction problems. International Journal of Mechanical Sciences 2007;49:183–99.
[6] Andersson, T. Boundary Elements in two dimensional contact and friction, Diss. No 85 Linköping Institute of Technology; 1982.
[7] Venturini WS, Brebbia CA. Some applications of the boundary element method in geomechanics. International Journal for Numerical and Analytical Methods in Geomechanics 1983;7(4):419–33.
[8] Man KW. Contact Mechanics using Boundary Elements. Topics in Engineering, vol. 22. Computational Mechanics Publication; 1994.
[9] Aliabadi MH. The Boundary Element Method, Vol 2: Applications in Solids and Structures. John Wiley & Sons Ltd; 2002.
[10] Gonzalez JA, Abascal R. Solving 2D rolling problems using the NORM-TANG iteration and mathematical programming. Computers and Structures 2000;78: 149–60.
[11] Chen TC, Chen WH. Frictional contact analysis of multiple cracks by incremental displacement and resultant traction boundary integral equations. Engineering Analysis with Boundary Elements 1998;21:339–48.
[12] Huesmann A, Kuhn G. Automatic load incrementation technique for plane elasto-plastic frictional contact problems using boundary element method. Computers and Structures 1995;56:733–45.
[13] Martin D, Aliabadi M. A BE hyper-singular formulation for contact problems using non-conforming discretization. Computers and Structures 1998;69: 557–65.
[14] Martin D, Aliabadi M. Boundary element analysis of two-dimensional elastoplastic contact problems. Engineering Analysis with Boundary Elements 1998;21:349–60.
[15] Paris F, Blazquez A, Cañas J. Contact problems with nonconforming discretizations using boundary element method. Computers and Structures 1995;57:829–39.
[16] Garrido JA, Forces A, Paris F. An incremental procedure for three-dimensional contact problems with friction. Computers and Structures 1994;50:201–15.
[17] González JA, Abascal R. Solving 2D transient rolling contact problems using the BEM and mathematical programming techniques. International Journal of Numerical Methods in Engineering 2002;53:843–75.
[18] Abascal R, Rodríguez-Tembleque L. Steady-state 3D rolling-contact using boundary elements. Communications Numerical Methods in Engineering 2007;33:905–20.
[19] Rodríguez-Tembleque L, Abascal R. A 3D FEM–BEM rolling contact formulation for unstructured meshes. International Journal of Solids and Structures 2010;47:330–53.
[20] Hong HK, Chen JT. Derivations of Integral equations of elasticity. Journal of Engineering Mechanics 1988;114(6):1028–44.
[21] Leonel ED, Venturini WS. Dual boundary element formulation applied to analysis of multi-fractured domains. Engineering Analysis with Boundary Elements 2010;34(12):1092–9.
[22] Partheymüller P, Haas M, Kuhn G. Comparison of the basic and the discontinuity formulation of the 3D-dual boundary element method. Engineering Analysis with Boundary Elements 2000;24:777–88.
[23] Benallal A, Botta AS, Venturini WS. On the description of localization and failure phenomena by the boundary element method. Computer Methods in Applied Mechanics and Engineering 2006;195:5833–56.
[24] Leonel ED, Venturini WS. Non-linear boundary element formulation with tangent operator to analyse crack propagation in quasi-brittle materials. Engineering Analysis with Boundary Elements 2010;34:122–9.
[25] Leonel ED, Chateauneuf A, Venturini WS, Bressolette P. Coupled reliability and boundary element model for probabilistic fatigue life assessment in mixed mode crack propagation. International Journal of Fatigue 2010;32:1823–34.
[26] Bonnet M, Mukherjee S. Implicit BEM formulation for usual and sensitivity problems in elasto-plasticity using the consistent tangent operator concept. International Journal of Solids and Structures 1996;33:4461–80.